

# $^1\text{H}$ , $^{13}\text{C}$ and $^{15}\text{N}$ backbone and side-chain assignment of a carbohydrate binding module from a xylanase from *Roseburia intestinalis*

Eva Madland<sup>1</sup>, Yoshihito Kitaoku<sup>2</sup>, Gerd Inger Sætrom<sup>1</sup>, Maria Louise Leth<sup>3</sup>, Morten Ejby<sup>3</sup>, Maher, Abou Hachem<sup>3</sup>, Finn Lillelund Aachmann<sup>1</sup>

<sup>1</sup> NOBIPOL, Department of Biotechnology and Food Science, NTNU Norwegian University of Science and Technology, Trondheim, Norway

<sup>2</sup> Department of Advanced Bioscience, Kinki University, Nara, Japan

<sup>3</sup> Department of Biotechnology and Biomedicine, Technical University of Denmark, Lyngby, Denmark

Corresponding author

Finn Lillelund Aachmann

E-mail: [finn.l.aachmann@ntnu.no](mailto:finn.l.aachmann@ntnu.no)

Phone number: +47 735 93 317

## Acknowledgements

This work was financed by SO-funds from NTNU, Norwegian University of Science and Technology and by the Norwegian NMR Platform and the KIFEE 2016-2018 program both from the Research Council of Norway (Grant Number 226244 and 249797), as well as Graduate School DTU Scholarship, Lyngby, Denmark and the Danish Research Council for Independent Research, Natural Sciences (DFF, FNU) by a Research Project 2 grant (Grant ID: 4002-00297B).

## Abstract

The N-terminal domain (residues 28-165) from the glycoside hydrolase family 10 from *Roseburia intestinalis* (RiCBMx), has been isotopically labeled and recombinantly expressed in *Escherichia coli*. Here we report <sup>1</sup>H, <sup>13</sup>C and <sup>15</sup>N NMR chemical shift assignments for this carbohydrate binding module (CBM).

### Keywords

Carbohydrate binding module (CBM), xylan binding module, xylanase, *Roseburia intestinalis*, gut microbiota

## Biological context

Most of the dietary fibers in the human diet comes from the plant cell walls present in fruits and vegetables. Here we find complex polysaccharides such as, cellulose, pectin and xylan (Koropatkin et al. 2012). The latter has a  $\beta$ -1,4-linked xylose backbone with varying degrees of polymerization and side-chain substitution (Rennie and Scheller 2014). Xylan can be substituted with carbohydrate side-chains, e.g. arabinofuranosyl and glucuronosyl residues or acetyl groups. A variety of linkages to side-chain residues necessitate the deployment of different enzymes for xylan degradation.

Members of the human gut microbiota (HGM) are able to ferment xylan into short-chain fatty acids (SCFAs) e.g. butyrate, propionate and acetate. Butyrate is known to have a beneficial effect on the host's health by being an energy source for colonocytes as well as reducing the risk of colon cancer and enteric colitis (Donohoe et al. 2012; Morrison and Preston 2016; Xu et al. 2017). As the population of butyrate-producers are more abundant in healthy individuals, there is a particular interest in the role they play in the HGM (Sheridan et al. 2016). One of the key known butyrate-producers from the HGM is *Roseburia*, a common genus in the clostridial cluster XIVa within Firmicutes (Louis and Flint 2009). *Roseburia intestinalis* has shown xylanolytic activity, and is together with species from *Bacteroides*, one of the few taxa that can utilize xylan (Chassard et al. 2007; Mirande et al. 2010). The ability of *Bacteroides* to degrade xylan have been investigated in detail (Martens et al. 2011; Rogowski et al. 2015; Zhang et al. 2014), but insight into the strategy used by Firmicutes to harvest energy from xylan has until recently been lacking.

A recent study (Leth et al. 2018) showed that *R. intestinalis* is able to breakdown xylan through a modular cell-attached xylanase of glycoside hydrolase family 10 (RiGH10A) that is conserved within the species. This enzyme is highly upregulated when *R.intestinalis* is grown on xylan and comprises of four xylan-binding modules: Two carbohydrate binding modules (CBMs) of family 9 (CBM9), one from family 22 (CBM22) and an N-terminal of a previously unknown family (CBMx). This representative of a new CBM family possesses low affinity for xylan, but displays selectivity for arabinoxylan, which makes it an interesting candidate for both structural and functional characterization studies by nuclear magnetic resonance (NMR).

## Methods and experiments

### Protein expression and purification

<sup>13</sup>C, <sup>15</sup>N and <sup>15</sup>N samples were expressed in *Escherichia coli* BL21 (DE3). Pre-culture was grown in LB medium (10 g/L tryptone, 5 g/L yeast extract and 5 g/L NaCl) supplemented with 10  $\mu$ L kanamycin (50 mg/mL) in a shaking incubator at 30 °C, 225 rpm overnight. From the pre-culture, 1 % (v/v) was used to inoculate 450 mL M9 media (6 g/L Na<sub>2</sub>HPO<sub>4</sub>, 3 g/L KH<sub>2</sub>PO<sub>4</sub>, 0.5 g/L NaCl) supplemented with 500  $\mu$ L kanamycin (50 mg/mL), 1 mL 1 M MgSO<sub>4</sub>, 10 mL Trace Metal solution (0.1 g/L ZnSO<sub>4</sub>, 0.8 g/L MnSO<sub>4</sub>, 0.5 g/L FeSO<sub>4</sub>, 0.1 g/L CuSO<sub>4</sub>, 1 g/L CaCl<sub>2</sub>), 5 mL Gibco™ MEM Vitamin Solution (100x), 10 mL <sup>15</sup>N Bioexpress Cell Growth Media (Cambridge Isotope Laboratories, Tewksbury, MA; USA), 2 g glucose (<sup>15</sup>N label)/ 98 % <sup>13</sup>C<sub>6</sub>-D-glucose (<sup>13</sup>C, <sup>15</sup>N label) in 20 mL milliQ. After inoculation the medium was supplemented 1 mL anti-foam and the cells were grown using Lex-24™

(Epiphyte) at 30 °C until  $OD_{600} = 0.8$ . The expression was induced with IPTG (isopropyl-1-thio- $\beta$ -D-galactopyranoside) to a final concentration of 1 mM, and incubated with Lex-24™ (Epiphyte) at 16 °C over night. The cells were harvested by centrifugation (Sorvall) at 4 °C, 6000  $\times$ g, 5 min. The pellet was resuspended in lysis buffer (50 mM  $NaH_2PO_4$ , 50 mM NaCl and 0.05 % TritonX-100) and ½ tablet cOmplete™ ULTRA protease inhibitor (Roche) in 20 mL milliQ, and sonicated using a Branson Sonifier equipped with a microtip for 10 minutes. Isolation of the lysate was done by centrifugation (Eppendorf) at 4 °C, 15 000  $\times$ g, for 2.5 h.

An Econo-Column® (Bio-Rad) containing 2 mL Ni-NTA Agarose (QIAGEN) was equilibrated with 20 column volumes WEB (50 mM  $Na_2HPO_4$ , 300 mM NaCl), pH 8.0. The lysate was incubated in the column for 45 minutes, and eluted with WEB with an increased amount of imidazole: 10 mM, 15 mM, 20 mM, 100 mM, 200 mM and 400 mM. Fractions containing CBMx were collected and purity confirmed with SDS-PAGE. To remove imidazole, the fractions were dialysed (MWCO 3.5 kDa) against 5 mM  $NaH_2PO_4$ , pH 5.5 over night.

To cleave the His-tag of the fraction containing CBMx, TEV-protease was added in 1/100 (w/w) and dialysed (MWCO 3.5 kDa) against 20 mM sodium phosphate, 1 mM DTT, 0.5 mM EDTA, pH 8.0. Purification of CBMx was done using a gravity flow column containing 2 mL cOmplete His-tag purification resin (Roche) equilibrated with the dialysis buffer. The dialyzed sample was applied to the column and the flow through was collected. The resin was washed with 1-5 column volumes of the same buffer and the sample was collected by combining this fraction with the flow through. Regeneration of the column was done with dialysis buffer containing 50 mM imidazole. An SDS-PAGE was run to confirm the separation and purity of the mature CBMx.

The CBMx containing fractions were concentrated and buffer exchanged into the NMR-buffer (50 mM sodium phosphate, pH 6.5. Samples for NMR was made with CBMx in NMR-buffer with  $D_2O$  added to a final ratio of 90 %  $H_2O$ /10 %  $D_2O$ ) by centrifugation using Vivaspin® 6 protein spin concentrators (MWCO 5 kDa, Sartorius) at 10 °C, 7000  $\times$ g.

## NMR spectroscopy

All CBMx NMR samples were prepared in 50 mM sodium phosphate buffer and 10 %  $D_2O$ , pH 6.5.

All spectra were recorded at 25 °C on a Bruker Ascend 800 MHz spectrometer Avance III HD Bruker Biospin equipped with a 5 mm Z-gradient CP-TCI (H/C/N) cryoprobe at the NV-NMR-Centre/Norwegian NMR Platform at NTNU Norwegian University of Science and Technology, Trondheim, Norway.  $^1H$  shifts were referenced internally to HDO, while  $^{13}C$  and  $^{15}N$  chemical shifts were referenced indirectly to HDO, based on the absolute frequency ratios (Zhang et al. 2003). Backbone and side-chain assignments of CBMx were elucidated using  $^{15}N$ -HSQC,  $^{13}C$ -HSQC, HNCA, HNcoCA, HNCO, HNcaCO, HNCACB, HNcoCACB, HNHAHB, HNcoHAHB and HcCH-TOCSY. The NMR data were recorded and processed with TopSpin version 3.5 and the data was analyzed with CARA version 1.5 (Keller 2004). Secondary structure elements were evaluated using TALOS-N (<https://spin.niddk.nih.gov/bax/software/TALOS-N/>) (Shen and Bax 2013) and chemical shifts of N,  $H^N$ ,  $C^\alpha$ ,  $C^\beta$ ,  $H^\alpha$ ,  $H^\beta$  and  $C'$ .

## Assignment and data deposition

Here we report the backbone and side-chain assignment of CBMx. Fig.1 shows the  $^{15}N$ -HSQC spectrum of CBMx together with the assigned resonances. The backbone assignment is essentially complete (N, HN,  $C^\alpha$ ,  $H^\alpha$  and  $C'$  > 98 %). The mature protein contains two extra amino acids (Gly-Ala) at the N-terminus (for purification purpose) that were only partially assigned. Side-chain assignment is almost complete (H and C side-chains >78 %). The overall percentage of completion is affected by the missing assignment of exchangeable side-chain protons of Arg, Lys, Asn and Gln as well as aromatic residues. Chemical shift data have been deposited at the Biological Magnetic Resonance Data Bank (BMRB) under the accession number 27536.

Analysis of the secondary structure elements (Fig. 2) indicates three  $\alpha$ -helices and ten  $\beta$ -sheets. A high degree of  $\beta$ -sheets is consistent with previously reported structures of carbohydrate binding modules. The typical  $\beta$ -sheet scaffold support the evolution of a variety of binding specificities and affinities in xylan-specific CBMs which merits further analyses.

## NOTES

### Ethical standards

The authors declare that the experiments described in this publication were done in compliance with the ethical standards of the countries in which they were performed.

### Conflict of interest

The authors declare that they have no conflict of interest.

## References

- Chassard C, Goumy V, Leclerc M, Del'homme C, Bernalier-Donadille A (2007) Characterization of the xylan-degrading microbial community from human faeces FEMS Microbiol Ecol 61:121-131 doi:10.1111/j.1574-6941.2007.00314.x
- Donohoe DR, Collins LB, Wali A, Bigler R, Sun W, Bultman SJ (2012) The Warburg effect dictates the mechanism of butyrate-mediated histone acetylation and cell proliferation Mol Cell 48:612-626 doi:10.1016/j.molcel.2012.08.033
- Keller R (2004) The Computer Aided Resonance Assignment (Goldau, Switzerland C Verlag (Ed)
- Koropatkin NM, Cameron EA, Martens EC (2012) How glycan metabolism shapes the human gut microbiota Nat Rev Microbiol 10:323-335 doi:10.1038/nrmicro2746
- Leth ML et al. (2018) Differential bacterial capture and transport preferences facilitate co-growth on dietary xylan in the human gut Nat Microbiol 3:570-580 doi:10.1038/s41564-018-0132-8
- Louis P, Flint HJ (2009) Diversity, metabolism and microbial ecology of butyrate-producing bacteria from the human large intestine FEMS Microbiol Lett 294:1-8 doi:10.1111/j.1574-6968.2009.01514.x
- Martens EC et al. (2011) Recognition and degradation of plant cell wall polysaccharides by two human gut symbionts PLoS Biol 9:e1001221 doi:10.1371/journal.pbio.1001221
- Mirande C, Kadlecikova E, Matulova M, Capek P, Bernalier-Donadille A, Forano E, Bera-Maillet C (2010) Dietary fibre degradation and fermentation by two xylanolytic bacteria *Bacteroides xyloisolvans* XB1A and *Roseburia intestinalis* XB6B4 from the human intestine J Appl Microbiol 109:451-460 doi:10.1111/j.1365-2672.2010.04671.x
- Morrison DJ, Preston T (2016) Formation of short chain fatty acids by the gut microbiota and their impact on human metabolism Gut Microbes 7:189-200 doi:10.1080/19490976.2015.1134082
- Rennie EA, Scheller HV (2014) Xylan biosynthesis Curr Opin Biotechnol 26:100-107 doi:10.1016/j.copbio.2013.11.013
- Rogowski A et al. (2015) Glycan complexity dictates microbial resource allocation in the large intestine Nat Commun 6:7481 doi:10.1038/ncomms8481
- Shen Y, Bax A (2013) Protein backbone and sidechain torsion angles predicted from NMR chemical shifts using artificial neural networks J Biomol NMR 56:227-241 doi:10.1007/s10858-013-9741-y
- Sheridan PO et al. (2016) Polysaccharide utilization loci and nutritional specialization in a dominant group of butyrate-producing human colonic Firmicutes Microb Genom 2:e000043 doi:10.1099/mgen.0.000043

- Xu S, Liu CX, Xu W, Huang L, Zhao JY, Zhao SM (2017) Butyrate induces apoptosis by activating PDC and inhibiting complex I through SIRT3 inactivation *Signal Transduct Target Ther* 2:16035  
doi:10.1038/sigtrans.2016.35
- Zhang H, Neal S, Wishart DS (2003) RefDB: A database of uniformly referenced protein chemical shifts *Journal of Biomolecular NMR* 25:173-195 doi:10.1023/a:1022836027055
- Zhang M et al. (2014) Xylan utilization in human gut commensal bacteria is orchestrated by unique modular organization of polysaccharide-degrading enzymes *Proc Natl Acad Sci U S A* 111:E3708-3717  
doi:10.1073/pnas.1406156111

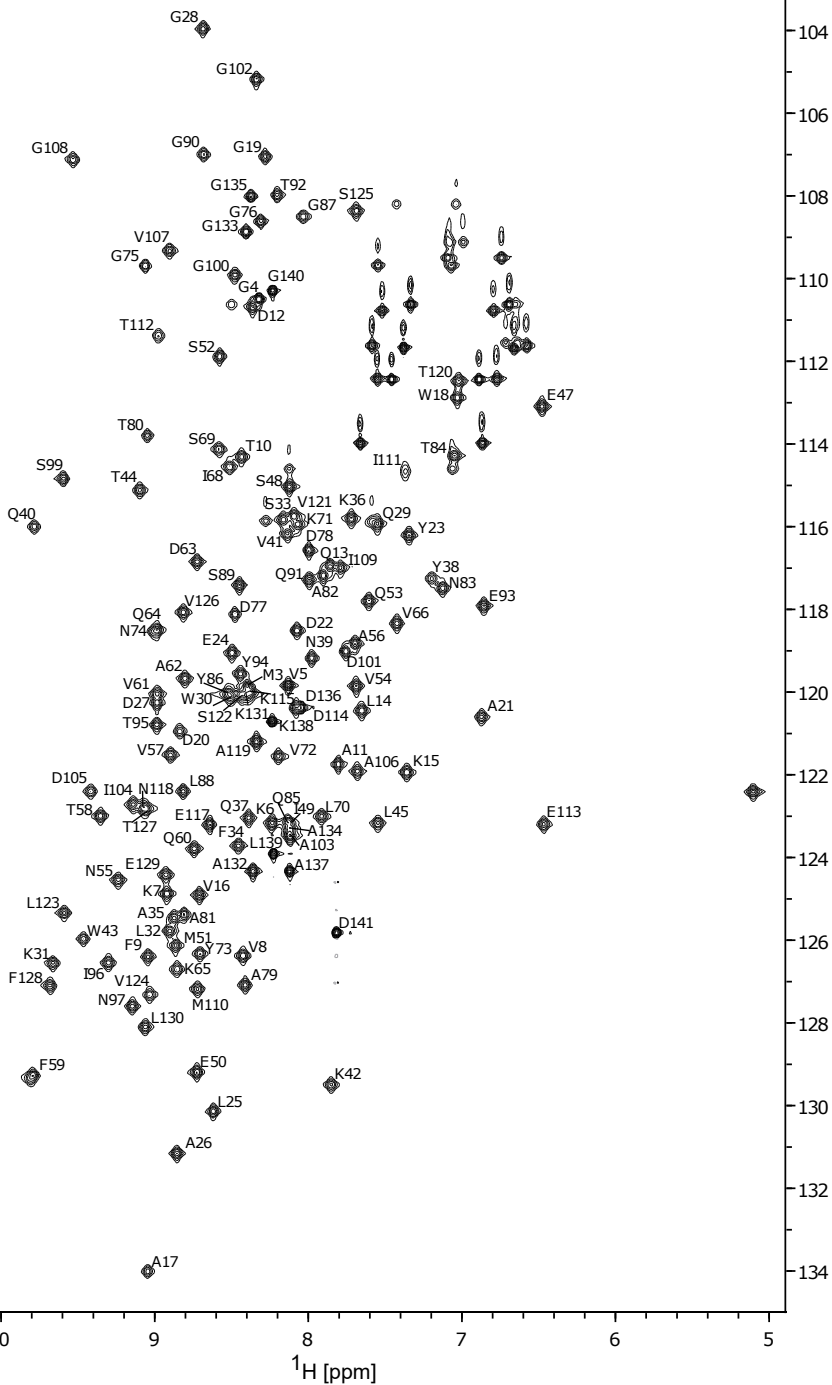


**Fig. 1**

$^1\text{H}$ ,  $^{15}\text{N}$  HSQC spectrum of  $^{13}\text{C}$ ,  $^{15}\text{N}$ -labeled CBMx (1.7 mM) from the glycoside hydrolase family 10 xylanase from *Roseburia intestinalis* (RiXyn10A) in 50 mM sodium phosphate, pH 6.5 with  $\text{D}_2\text{O}$  added to a final ratio of 90 %  $\text{H}_2\text{O}$ /10 %  $\text{D}_2\text{O}$ . Residue number and type are indicated on the figure

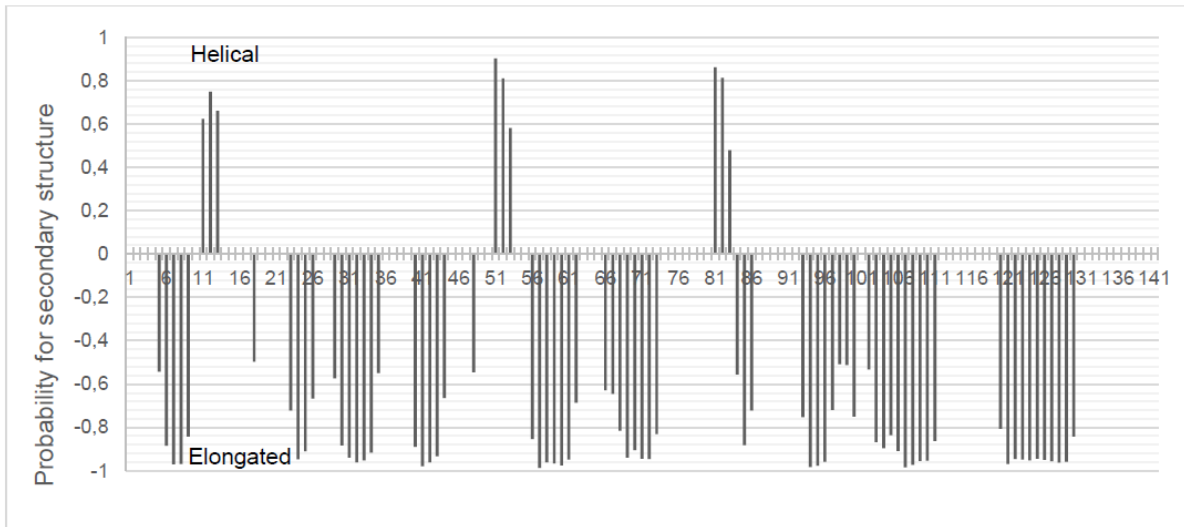


**Fig. 2**

Secondary structure probability of CBMx using TALOS-N. The probability of helical structure is shown as positive values, while negative values are used for the probability of an elongated structure